

## Electrochemical Behaviour of a Series of Iron(II), Nickel(II) and Copper(II) Complexes with Linear Pentadentate Schiff-Base Ligands

P. ZANELLO, R. CINI and A. CINQUANTINI

Istituto di Chimica Generale dell'Università, Piano dei Mantellini 44, 53100 Siena, Italy

Received March 10, 1983

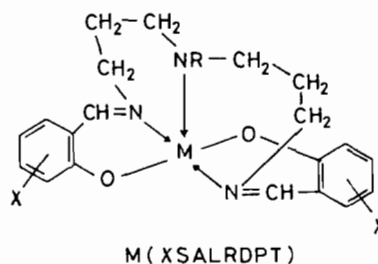
The electrochemical behaviour of iron(II), nickel(II) and copper(II) complexes with a number of derivatives of the pentadentate ligand bis(salicylideneimine-3-propyl)amine (*X*-SALRDPT) has been investigated in non-aqueous solvent. The one-electron anodic oxidation of all the metal(II) complexes has been characterized and correlated, as well as the frequency shifts of their *d*–*d* transitions, to the inductive effect of the various substituents on the salicylic moieties. Crystal field stabilization energies involved in the redox change are discussed. The cathodic charge transfers II/I and I/0 for nickel(II) and copper(II) chelates have been also investigated. On the basis of electrochemical measurements, some considerations on the reactivity of the complexes towards dioxygen are made.

### Introduction

Understanding the way dioxygen interact with a metal ion is important for both biological and commercial systems. A few naturally occurring molecules capable to bind dioxygen are known, but owing to their complexity simple compounds which exhibit the important oxygen-carrying property have been synthesized and investigated by several techniques in recent years.

The ligand bis(salicylideneimine-3-propyl)amine and its derivatives form pentadentate complexes with cobalt(II) [1–3] and iron(II) [4] ions able to react with dioxygen. The results from a number of studies including EPR, IR and single crystal X-ray diffraction have been used to get information about the electronic charge on the metal center, both in the oxygenated species and in the precursors. Since electrochemical techniques have shown to be an useful tool to investigate the correlation between the redox potentials of the cobalt(II) centre in this type of complexes and the ability to react with dioxygen [2], we have now extended such

kind of investigation to a wider series of these  $M(XSALRDPT)$  complexes.



R = H, Me

X = H, 3-MeO, 4-MeO, 5-MeO, 5-Cl, 5-NO<sub>2</sub>

M = Fe, Cu, Ni

### Experimental

#### Materials

Ferrous sulfate ( $FeSO_4 \cdot 7H_2O$ ), copper acetate ( $Cu(CH_3COO)_2 \cdot H_2O$ ) and nickel acetate ( $Ni(CH_3COO)_2 \cdot 4H_2O$ ) were reagent grade Merck products.

Bis(3-aminopropyl)amine (DPT), 2-hydroxybenzaldehyde (HSAL), 2-hydroxy-4-methoxybenzaldehyde (4-MeO-SAL) were purchased from Aldrich; bis-(3-aminopropyl)methylamine (MeDPT), 5-chloro-2-hydroxybenzaldehyde (5-Cl-SAL), 2-hydroxy-3-methoxybenzaldehyde (3-MeO-SAL) and 2-hydroxy-5-methoxybenzaldehyde (5-MeO-SAL) were purchased from ICN (K & K); 2-hydroxy-5-nitrobenzaldehyde (5-NO<sub>2</sub>-SAL) was a Merck product.

Ferrous acetate ( $Fe(CH_3COO)_2 \cdot 4H_2O$ ) was obtained by dissolving iron turnings in a deaerated acetic acid solution. The solid was precipitated by evaporation under vacuum in a stream of ultrapure nitrogen.

Dimethylsulfoxide solvent (DMSO), as well as tetraethylammonium perchlorate supporting electrolyte ( $[NEt_4][ClO_4]$ ), were prepared as previously described [2].

### Preparation of the Complexes

Copper(II) and nickel(II) complexes were prepared according to literature procedures [5]. Iron(II) derivatives were obtained according to Ref. 4 and starting from ferrous acetate following the procedure in Ref. 5.

### Apparatus and Methods

The electrochemical apparatus used here has been previously described [2]. All potential values refer to an aqueous saturated calomel electrode (SCE). The temperature was controlled at  $20 \pm 0.1$  °C. Cyclic voltammetric current-potential curves have been analysed as a function of the scan rate [6],  $v$ , on the basis of: the anodic, or cathodic peak potential ( $E_p^a$ , or  $E_p^c$ ), the difference between the peak potential value of a response and that of the reverse one [ $(E_p^a - E_p^c)$  for an anodic process, or  $(E_p^c - E_p^a)$  for a cathodic process], the quotient of the peaks current of the reverse and the direct response [ $(i_p^c/i_p^a)$  for an anodic process, or  $(i_p^a/i_p^c)$  for a cathodic process], the quotient of the peak current of the response and the square root of the scan rate ( $i_p/v^{1/2}$ ).

In cyclic voltammetry the number of electrons involved in the electrode processes has been evaluated by comparison with the one-electron oxidation of ferrocene.

The U.V. and visible absorption spectra were recorded with a Model 200 Perkin-Elmer spectrophotometer connected with a Model 56 recorder by using 1-cm quartz cells. Reflectance spectra were measured on powdered samples.

## Results and Discussion

### Nickel(II) Derivatives

In DMSO solution all the nickel(II) complexes studied undergo, at a platinum electrode, an anodic process which gives cyclic voltammetric responses consisting of an anodic-cathodic peak system. As an example the cyclic voltammogram reported in Fig. 1b illustrates the anodic behaviour of a solution of Ni(5-Cl-SALDPT).

The significant features of the cyclic voltammetric responses have been analysed as a function of the scan rate in the range from 0.02 to 100  $V s^{-1}$ . The results of this analysis indicate that the anodic oxidation of Ni(X-SALRDPT) derivatives involves a one-electron quasi-reversible charge transfer in all cases except for X = 3-MeO, 5-MeO, where the electrode process is complicated by chemical reactions following the charge transfer. The use of fast potential scan rates prevents the chemical complications coupled to the electron transfer, so that these compounds also undergo an uncomplicated one-electron oxidation process at scan rates higher than 10  $V s^{-1}$ .

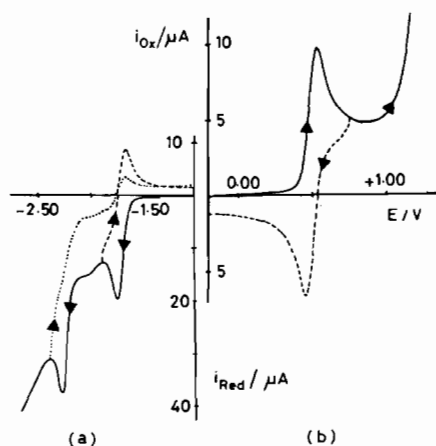
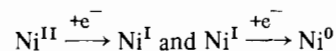


Fig. 1. Cyclic voltammetric responses of a DMSO solution containing Ni(5-Cl-SALDPT) ( $1.60 \times 10^{-3}$  mol  $dm^{-3}$ ) and  $[NEt_4][ClO_4]$  (0.1 mol  $dm^{-3}$ ). a) Cathodic scan; mercury working microelectrode. b) Anodic scan; platinum working microelectrode. Scan rate: 0.2  $V s^{-1}$ .

All nickel(II) derivatives also display cathodic responses at both platinum and mercury electrodes. Cyclic voltammetry at a mercury electrode shows the presence of two successive reduction processes; at a platinum electrode the more cathodic step is masked by the solvent discharge. In the case of the nitro-compounds the electroreduction of the  $NO_2$  group interferes. In Fig. 1a the cathodic behaviour of Ni(5-Cl-SALDPT) is reported as a typical example.

The analysis of the responses at different scan rates allows us to state that the less cathodic process involves a one-electron quasi-reversible charge transfer, complicated by coupled following chemical reactions, while the more cathodic process consists of an irreversible one-electron charge transfer. The two steps can be formally attributed to the



charge transfers, respectively. In the hypothesis that the involved quasi-reversible charge transfers proceed with transfer coefficients ranging from 0.3 to 0.7, the reversible half-wave potential,  $E_{1/2}^r$ , which can be assumed as the formal electrode potential,  $E^{o'}$ , can be computed as the average of the cathodic (or anodic) peak potential and the directly associated anodic (or cathodic) peak potential, and the heterogeneous rate constant at the standard potential of the redox couples,  $k_s$ , can be roughly evaluated by Nicholson's treatment [7], under some previously described assumptions [2].

Experiments at different Ni(II) concentrations showed the  $Ni^{II} \rightarrow Ni^I$  charge transfer to be followed by a first-order irreversible chemical reaction. The half life of the electrogenerated Ni(I) species can be approximately evaluated through the working

TABLE I. Electrochemical Characteristics of the Following Charge Transfers: (a)  $\text{Ni(II)} \xrightarrow{-e^-} \text{Ni(III)}$  at Platinum Electrodes; (b)  $\text{Ni(II)} \xrightarrow{+e^-} \text{Ni(I)}$  and (c)  $\text{Ni(I)} \xrightarrow{+e^-} \text{Ni(0)}$  at Mercury Electrodes.

Ni(II) complex	(a)		(b)			(c) $E_p^{**}/V$
	$E^{\circ'}/V$	$k_s/cm \text{ sec}^{-1}$	$E^{\circ'}/V^*$	$k_s/cm \text{ sec}^{-1}$	$t_{1/2}/\text{sec}$ for Ni(I) complex	
H-SALDPT	+0.41	$1.4 \times 10^{-2}$	-1.68	—	0.06	-2.50
5Cl-SALDPT	+0.50	$1.2 \times 10^{-2}$	-1.70	—	0.03	-2.30
5NO <sub>2</sub> -SALDPT	+0.76	$0.9 \times 10^{-2}$	—	—	—	—
3MeO-SALDPT	+0.35	$1.8 \times 10^{-2}$	-1.69	—	0.06	—
5MeO-SALDPT	+0.36	$1.9 \times 10^{-2}$	-1.79	—	0.12	-2.48
H-SALMeDPT	+0.44	$1.8 \times 10^{-2}$	-1.76	$0.7 \times 10^{-2}$	1.38	-2.53
5Cl-SALMeDPT	+0.54	$2.0 \times 10^{-2}$	-1.71	$1.0 \times 10^{-2}$	1.98	-2.31
5NO <sub>2</sub> -SALMeDPT	+0.83	$0.7 \times 10^{-2}$	—	—	—	—
3MeO-SALMeDPT	+0.41	$1.6 \times 10^{-2}$	-1.71	$1.6 \times 10^{-2}$	4.33	-2.56
5MeO-SALMeDPT	+0.38	$1.2 \times 10^{-2}$	-1.77	$0.5 \times 10^{-2}$	4.07	-2.48

\*Values at scan rates in which the  $i_p^a/i_p^c$  ratio reaches unity, indicating the overcoming of the complications from coupled chemical reactions. \*\*Peak potential values at  $v = 0.2 \text{ V s}^{-1}$ .

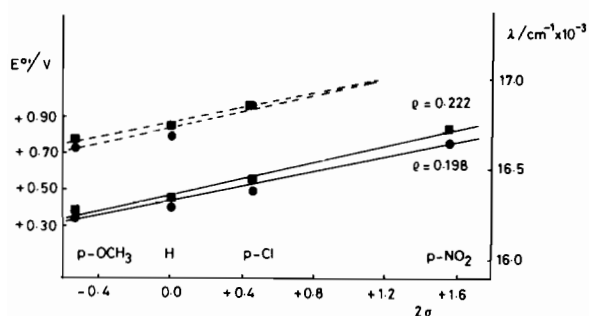


Fig. 2. Linear regression analysis of the dependence of the oxidation potential (solid lines) and of the d-d transition frequencies (dashed lines) of the nickel(II) complexes on the sum of the Hammett substituent constants,  $2\sigma$ . (●) SALDPT and (■) SALMeDPT derivatives.

curve of the trend of the anodic to cathodic currents ratio as a function of  $\log(k\tau)$  [8], where  $k$  is the rate constant of the chemical reaction coupled to the charge transfer and  $\tau$  is the time spent in going from  $E_{1/2}$  to the switching potential.

Table I summarizes the most significant parameters for the electrode behaviour of nickel(II) complexes. The  $k_s$  value for the reduction process of SALDPT derivatives could not be calculated, because at scan rates where the chemical complications coupled to the charge transfer are prevented ( $i_p^a/i_p^c = 1$ ) the peak separation is too high to apply Nicholson's technique.

Half-life values indicate Ni(I)(SALMeDPT) derivatives to be more stable than the corresponding SALDPT ones.

The formal potentials appear sensitive to electronic effects of the phenyl substituents. For the oxidation process the Hammett relationship holds\* (Fig. 2, solid lines) if one considers the 3-, 4-, 5-substituents to be *ortho*, *meta*, *para*, respectively, with respect to the phenolic oxygen atom [2]. In the case of the  $\text{Ni(II)} \rightarrow \text{Ni(I)}$  reduction the set of available data is too incomplete to be considered.

As previously pointed out [2], it must be concluded that in this class of compounds the electron density on the metal center is enhanced or diminished by phenyl substituents *via* the Ph-O-M-O-Ph pathway. This conclusion could be also inferred by studying the frequency shifts of the d-d transitions of the same complexes as functions of the Hammett substituent constants. In fact, as shown in Fig. 2 by the dashed lines, the frequency patterns in DMSO solution are similar to those of the oxidation potentials. In a less coordinating solvent like benzene, Hammett relations are followed even better.

The spectra of Ni(X-SALRDPT) complexes are in agreement with a distorted trigonal bipyramidal stereochemistry [9, 10]. In this assumption the

\*In the case of a ligand having two substituents, the Hammett relationships become:  $\Delta \log K = 2\sigma\rho$ ,  $\Delta E_{1/2} = 2\sigma\rho E_{MF}$ .

TABLE II. Electrochemical Significant Parameters of the Following Charge Transfers: (a)  $\text{Cu(II)} \xrightarrow{-e^-} \text{Cu(III)}$  at a Platinum Electrode; (b)  $\text{Cu(II)} \xrightarrow{+e^-} \text{Cu(I)}$  and (c)  $\text{Cu(I)} \rightarrow \text{Cu(0)}$ , at a Mercury Electrode.

Cu(II) complex	(a)	(b)		(c)
	$E^{\circ'}/\text{V}$	$E^{\circ'}/\text{V}$	$t_{1/2}/\text{sec}$ for Cu(I) complex	$E_p^*/\text{V}$
H-SALDPT	+0.84*	-1.06	2.8	-1.50
5Cl-SALDPT	+0.69	-0.96	1.7	-1.35
5NO <sub>2</sub> -SALDPT	—	-0.80*	—	-1.05
3MeO-SALDPT	+0.43	-1.05	5.1	-1.62
5MeO-SALDPT	+0.47	-1.07	2.3	-1.55
H-SALMeDPT	+0.71	-1.02	7.7	-1.46
5Cl-SALMeDPT	+0.80	-0.94	6.8	-1.55
5NO <sub>2</sub> -SALMeDPT	—	-0.73*	—	—
3MeO-SALMeDPT	+0.55	-1.00	38	-1.65
5MeO-SALMeDPT	+0.54	-1.02	13	-1.50

\*Potential peak value at  $v = 0.2 \text{ V s}^{-1}$ .

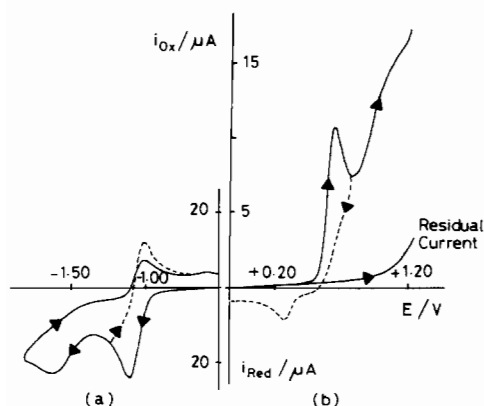


Fig. 3. Cyclic voltammograms recorded on a DMSO solution containing  $\text{Cu(3MeOSALDPT)}$  ( $1.27 \times 10^{-3} \text{ mol dm}^{-3}$ ) and  $[\text{NEt}_4][\text{ClO}_4]$  ( $0.1 \text{ mol dm}^{-3}$ ). a) Cathodic scan; mercury working microelectrode. b) Anodic scan; platinum working microelectrode. Scan rate  $0.2 \text{ V s}^{-1}$ .

selected absorptions are likely to be attributable to  ${}^3E' \rightarrow {}^3A_2'$  transition. This assignment agrees with the red-shift observed for electron donating substituents. It practically corresponds to an electron displacement from  $d_{x^2-y^2}$  or  $d_{xy}$  orbitals (enriched in negative charge by phenolic oxygen donors) to  $d_{z^2}$  orbital (not influenced by substituents on the salicylic moieties). It is interesting that the frequencies, as well as the trend of their shifts as a function of salicylic substituents, are practically

the same in the solid state and in solution for all the complexes, except  $\text{Ni(5-NO}_2\text{-SALRDPT)}$ .

The bubbling of dioxygen in DMSO solutions of  $\text{Ni(X-SALRDPT)}$  complexes causes no reaction in accordance with their rather high oxidation potentials.

#### Copper(II) Derivatives

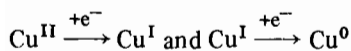
In Fig. 3 the cyclic voltammetric behaviour of copper(II)-(X-SALRDPT) derivatives in DMSO is outlined, taking  $\text{Cu(3-MeO-SALDPT)}$  as a typical example.

As can be seen from Fig. 3b, the anodic process involves a first step with a low degree of reversibility and a subsequent one, irreversible in character and close to the solvent discharge, attributable to the oxidation of the ligand. The analysis of the responses as a function of the scan rate indicates that the first anodic process involves a charge transfer followed by both chemical complications and charge transfers (e.c.e. mechanism). This behaviour is rather usual with anodic oxidations of copper(II) complexes involving both the metal center and the ligand [11–15].

Cyclic voltammetric data at scan rates ranging from  $20$  to  $50 \text{ V s}^{-1}$  allow us to evaluate the formal potentials for the one-electron metal ion oxidation, except for both  $\text{Cu(SALDPT)}$ , the electrode process of which appears irreversible in character, and  $5\text{NO}_2$  derivatives, which are oxidized at potential values beyond the range of the solvent. The low degree of reversibility of the first charge-transfer does not allow

to compute the heterogeneous charge-transfer constant; only in the case of Cu(5-MeO-SALDPT) has it been possible to obtain a value of  $9.0 \times 10^{-3} \text{ cm sec}^{-1}$ .

The electroreduction of Cu(X-SALRDPT) derivatives at mercury electrodes involves two successive one-electron charge transfers, formally attributable to the



steps (Fig. 3a). As in the case of nickel(II) derivatives, the first step involves a quasi-reversible charge transfer coupled to a subsequent chemical reaction, which can be prevented in all cases by using scan rates higher than  $2-5 \text{ V s}^{-1}$ . The second step, irreversible in character, leads to  $\text{Cu}^0$  complex species which are re-oxidized at  $\sim -0.7 \text{ V}$ . This indicates that no decomposition to copper metal occurs in the voltammetric time scale ( $E_{1/2} \text{ Cu}^{\text{I}}/\text{Cu}^0$  in DMSO =  $-0.12 \text{ V}$  [16]).

In Table II the potentials of the above described charge transfers are reported, together with an approximate value of the half-life of the electro-generated Cu(I) complex species.

Like Ni(I) derivatives, Cu(I)(SALMeDPT) complexes are more stable than the corresponding SALDPT ones. Also in this case a linear correlation holds between the oxidation potentials of Cu(X-SALRDPT) derivatives and the sum of the Hammett substituent constants. An  $E^{\circ'}$  value of  $+1.10 \text{ V}$  can be computed for the oxidation potential of Cu(5-NO<sub>2</sub>SALMeDPT). The value of the reaction constant,  $\rho = 0.264$ , indicates that the ease of oxidation of copper(II) SALMeDPT derivatives is sensitive to electronic effects to about the same extent as the corresponding nickel(II) compounds. As in the case of Ni(II) derivatives, electronic effects seem less significant for the first cathodic process  $\text{Cu}^{\text{II}} \rightarrow \text{Cu}^{\text{I}}$ . Again a linear correlation holds between visible absorption frequencies of the copper(II) compounds and the Hammett constants of the salicylic substituents. The bands selected were those at about  $12,000 \text{ cm}^{-1}$ , attributable to the  ${}^2A_1' \rightarrow {}^2E''$  transition in which an electron is promoted from a xz or yz orbital (more influenced by the charge on the phenolic oxygen) to the  $d_{z^2}$  orbital [10] interacting with N(1) and N(2) atoms. In fact, the coordination sphere in the CuXSALRDPT complexes is likely a distorted trigonal bipyramid, in analogy with similar species Cu(mbp), in which the O-Cu-O equatorial angle is about  $152^\circ$  [17].

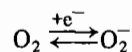
As expected on the basis of their oxidation potentials Cu(X-SALRDPT) complexes do not react with dioxygen.

#### Iron(II) Derivatives

In cyclic voltammetry both at mercury and platinum electrodes the anodic response of iron(II)

X-SALRDPT complexes appeared as a well-formed peak, with a cathodic peak directly associated in the reverse scan. In all cases ill-defined processes were present in the cathodic region at potential values more negative than  $-2.3 \text{ V}$ . The treatment of cyclic voltammetric data indicates that the anodic process involves a simple quasi-reversible one-electron charge transfer. The significant parameters of the anodic charge transfer relevant to Fe(X-SALRDPT) derivatives are reported in Table III. As in previous cases the oxidation potential of Fe(II) derivatives is linearly correlated to the inductive effects of electron withdrawing and electron donating groups present in the phenyl rings of the ligand. The values of the reaction constant ( $\rho = 0.130$  and  $0.115$  for SALMeDPT and SALDPT derivatives, respectively) point to a lower sensitivity to electronic effects in comparison with Ni(II) and Cu(II) analogous compounds.

Upon oxygenation performed by bubbling dry oxygen for 30 min in a deaerated Fe(5-NO<sub>2</sub>-SALMeDPT) solution the following voltammetric picture was observed: a) the initial anodic peak,  $E^{\circ'} = -0.04 \text{ V}$ , lowered up to the height relevant to the amount of Fe(II) derivative in excess, if any, in respect to the O<sub>2</sub> concentration; b) in the cathodic region a few reduction processes (not well-shaped) appeared at potentials more positive than the oxygen to superoxide ion reduction ones; c) the catho-anodic system of the



charge transfer showed an  $i_p^a/i_p^c$  ratio of about 0.6, indicating that species able to react with free superoxide ions were present in solution.

TABLE III. Electrochemical Characteristics of the Fe(II)  $\xrightarrow{-e^-} \text{Fe(III)}$  Charge Transfer at a Mercury Electrode.

Fe(II) complex	$E^{\circ'}/\text{V}$	$k_s/\text{cm sec}^{-1}$
H-SALDPT	-0.29	$2.0 \times 10^{-2}$
5Cl-SALDPT	-0.25	$1.6 \times 10^{-2}$
5NO <sub>2</sub> -SALDPT	-0.10	$2.1 \times 10^{-3}$
3MeO-SALDPT	-0.31	$4.1 \times 10^{-2}$
4MeO-SALDPT	-0.32	$5.6 \times 10^{-3}$
5MeO-SALDPT	-0.33	$1.7 \times 10^{-2}$
H-SALMeDPT	-0.25	$2.0 \times 10^{-2}$
5Cl-SALMeDPT	-0.20	$1.7 \times 10^{-2}$
5NO <sub>2</sub> -SALMeDPT	-0.04	$2.0 \times 10^{-2}$
3MeO-SALMeDPT	-0.26	$3.5 \times 10^{-2}$
4MeO-SALMeDPT	-0.29	$7.0 \times 10^{-3}$
5MeO-SALMeDPT	-0.30	$4.0 \times 10^{-3}$

By subsequent nitrogen bubbling for 30 min, in order to remove free oxygen, the following voltammetric picture was observed: a) no Fe(II) initial derivative was restored, indicating the oxygenation reaction to be an irreversible process; b) in the cathodic region up to  $-1.2$  V, where the reduction of the nitro group occurs, a few ill defined reduction processes were still present, the most important and the best shaped cathodic peak being located at  $-0.23$  V.

Controlled potential electrolysis at a mercury pool at  $-1.1$  V showed a consumption of one electron per iron atom contained in the oxygenated species. At the end of the electrolysis the voltammetric response showed that cathodic processes were no larger present, and a new anodic-cathodic peak system was formed ( $E^{o'} = -0.20$  V), attributable to a Fe(II) compound different from the precursor. This peak system is hence due to the reduced form of the major species formed by oxygenation ( $E_p^c = -0.23$  V).

U.V.-visible spectra recorded at the different stages of the oxygenation were as follows: a) Fe(5-NO<sub>2</sub>-SALMeDPT) in deaerated DMSO absorbs at 390 and 490 nm; b) upon oxygenation and subsequent deaeration absorption occurs at 360 nm with a shoulder at 490 nm; c) the solution from exhaustive electrolysis at  $-1.1$  V absorbs at 390 and 490 nm, no other peaks being observed up to 900 nm.

Niswander and Martell [4] have identified the oxygenation product of Fe(5-NO<sub>2</sub>-SALMeDPT) as the  $\mu$ -oxo compound [Fe<sup>III</sup>(5-NO<sub>2</sub>-SALMeDPT)]<sub>2</sub>O.

The similarity between the two spectra described in the points a) and c) seems to indicate that the electrolytic process is able to regenerate the precursor. However this conclusion is not in agreement with the voltammetric tests on the electrolyzed solutions. On the other hand it must be pointed out that some iron(II) complexes with pseudo-octahedral coordination stereochemistry in low spin or spin equilibrium states show an absorption pattern similar to that described under point c), both in the energies and in the relative intensities [18–20]. It hence seems plausible to suppose that the electroreduction of the iron(III)  $\mu$ -oxo compound simply leads to the corresponding iron(II) derivative. A formal potential of  $-0.20$  V can be attributed to this redox couple.

We do not know if one species of the  $\mu$ -oxo redox couple or some by-product is responsible for the reaction with electrogenerated superoxide ion; it seems plausible to suppose that some unrecovered amount of Fe(III) starting complex formed reacts with superoxide ions to give the superoxo species Fe<sup>III</sup>(5-NO<sub>2</sub>-SALMeDPT)O<sub>2</sub>.

The study of the oxygenation process of other Fe(X-SALRDPT) derivatives led to different results.

TABLE IV. Approximate Rate Constant Values of the Reaction Following the Superoxide Ions Electrogeneration (sec<sup>-1</sup>).

R	5NO <sub>2</sub>	H	5Cl	3MeO	4MeO	5MeO
SALMeDPT	3.0	0.4	1.6	0.6	0.5	0.2
SALDPT	1.5	0.4	0.2	0.4	0.4	0.2

The behaviour of Fe(5-MeO-SALMeDPT) is reported as a typical example. After bubbling oxygen for 30 min the following voltammetric picture appeared: the initial anodic response,  $E^{o'} = -0.30$  V, was no longer present; at potentials more negative than that of the catho-anodic system O<sub>2</sub>  $\rightleftharpoons$  O<sub>2</sub><sup>-</sup> two cathodic peaks appeared ( $E_{pc} = -1.08$  and  $-1.90$  V, respectively). Also in this case electrogenerated superoxide ions, although to a minor extent ( $i_p^a/i_p^c = 0.8$ ), undergo a subsequent chemical reaction. After deaeration by bubbling nitrogen for 30 min no anodic process regenerated, while the two cathodic processes were still detectable.

Controlled potential coulometric tests on a mercury pool at  $-1.25$  V showed the consumption of about one-half mol of electrons per mol of starting compound. Cyclic voltammetry at the end of the electrolysis revealed that the cathodic peak at  $-1.90$  V was still present and the initial anodic peak partially restored. By completing the electrolysis at  $-1.9$  V an overall consumption of one mol of electrons per mol of starting compound occurred. Cyclic voltammetry after exhaustive electrolysis revealed also the presence of a new anodic process at  $+0.05$  V from the anodic oxidation of an electrogenerated Fe(II) species different from the starting one.

The identification of the oxygenation products is a very difficult problem [4]. However the present electrochemical investigation at least suggests some remarks: a) it seems possible that two major oxygenated Fe(III) species,  $\mu$ -oxo and  $\mu$ -peroxo Fe(III) derivatives, may be formed. In addition, from an irreversible decomposition, some amounts of mononuclear Fe(III) compound arise, able to react with electrogenerated superoxide ions to give the relevant superoxo species. Even if  $\mu$ -peroxo diiron(III) complexes are generally thought to be stable at low temperature, a  $\mu$ -peroxo Fe(III) species of a macrocyclic pentadentate ligand stable at room temperature has been recently reported [21]; b) the voltammetric picture is consistent however with the predominant formation of the only  $\mu$ -oxo derivative, the two reduction peaks being attributable to the two Fe(III) centres. The rather high  $\Delta E$  value (0.8 V) is not unusually large if one considers that oxo-bridged ruthenium complexes [(NH<sub>3</sub>)<sub>5</sub>Ru-O-

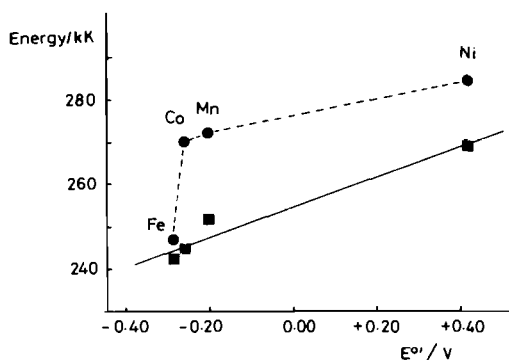
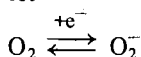


Fig. 4. Third ionization energies vs. the oxidation potentials of M(HSALDPT) derivatives, where M = Fe, Co, Mn, Ni (dashed line). Values corrected for c.f.s.e. (solid line).

$\text{Ru}(\text{NH}_3)_5]^{5+}$  and  $\text{Cl}(\text{bpy})_2\text{Ru}-\text{O}-\text{Ru}(\text{bpy})_2\text{Cl}]^{3+}$  show  $\Delta E$  values of 2.0 V [22] and 2.2 V [23], respectively, large value of  $\Delta E$  indicating high stability of the mixed valence systems [24]; c) contrary to Co(X-SALMeDPT) derivatives [2], the corresponding Fe(II) species do not react reversibly with dioxygen.

By assuming an irreversible pseudo-first order chemical reaction to be involved in the consumption of electrogenerated superoxide ions, the rate constant  $k$  of the chemical reaction following the charge transfer



can be calculated [8] (see Table IV). Only in the case of 5-Cl derivatives is there an important difference in the rate constants between SALMeDPT and SALDPT species.

Finally, it is interesting to compare the redox process +2/+3 in the gas phase, expressed by the third ionization energy of the elements, with the same redox change in solution, where the metal ions are complexed by the ligand, expressed by the oxidation potentials for X-SALRDPT derivatives, taking into account literature data for Mn compounds too [25]. As an example, in Fig. 4 the third ionization energies of the metals (dashed line) are plotted *versus* the oxidation potentials of H-SALDPT derivatives. As can be noted the two parameters do not increase linearly. However, if we apply the appropriate corrections for the gain in energy due to crystal field stabilization [26–28]\* a reasonably good linear trend is obtained (the correlation coefficient of the solid line in Fig. 4 is 0.98) although solvation energies of the divalent and trivalent ions have not been considered. This should

\*For the Ni(II) and Ni(III) derivatives the following parameters have been computed:  $Dq_{\text{oh}} = 1100$  and  $2000 \text{ cm}^{-1}$ , respectively.

indicate that in complexes of trigonal bipyramidal stereochemistry the gain in crystal field stabilization energy (c.f.s.e.) experienced in redox changes follows the order  $d^7/d^6 \cong d^5/d^4 > d^8/d^7 \gg d^6/d^5$ .

### Acknowledgements

Financial support by Italian C.N.R. is gratefully acknowledged.

### References

- 1 R. H. Niswander and L. T. Taylor, *J. Am. Chem. Soc.*, **99**, 5935 (1977).
- 2 P. Zanello, R. Cini, A. Cinquantini and P. Orioli, *J. Chem. Soc., Dalton Trans.*, in press.
- 3 R. Cini and P. Orioli, *J. Chem. Soc., Chem. Commun.*, 196 (1981).
- 4 R. H. Niswander and A. E. Martell, *Inorg. Chem.*, **17**, 1511 (1978).
- 5 L. Sacconi and I. Bertini, *J. Am. Chem. Soc.*, **88**, 5180 (1966).
- 6 E. R. Brown and R. F. Large, 'Physical Methods of Chemistry, Part IIA, Electrochemical Methods', A. Weissberger, B. W. Rossiter Eds., Wiley-Interscience, New York (1971) Vol. 1, p. 423.
- 7 R. S. Nicholson, *Anal. Chem.*, **37**, 1351 (1965).
- 8 R. S. Nicholson and I. Shain, *Anal. Chem.*, **36**, 706 (1964).
- 9 M. Di Vaira, P. Orioli and L. Sacconi, *Inorg. Chem.*, **10**, 553 (1971).
- 10 J. S. Wood, *Progress in Inorganic Chemistry*, **16**, 227 (1972).
- 11 A. Cinquantini, R. Cini, R. Seeber and P. Zanello, *J. Electroanal. Chem.*, **121**, 301 (1981).
- 12 A. Cinquantini, R. Seeber, R. Cini and P. Zanello, *J. Electroanal. Chem.*, **134**, 65 (1982).
- 13 P. Zanello, R. Seeber, A. Cinquantini, G. A. Mazzocchin and L. Fabbrizzi, *J. Chem. Soc., Dalton Trans.*, 893 (1982).
- 14 P. Zanello, P. A. Vigato and G. A. Mazzocchin, *Transition Metal Chem.*, **7**, 291 (1982).
- 15 L. Fabbrizzi, A. Poggi and P. Zanello, *J. Chem. Soc., Dalton Trans.*, in press.
- 16 J. N. Butler, *J. Electroanal. Chem.*, **14**, 89 (1967).
- 17 P. C. Healy, G. M. Mockler, D. P. Freyberg and E. Sinn, *J. Chem. Soc., Dalton Trans.*, 691 (1975).
- 18 J. P. Jesson, S. Trofimenko and D. R. Eaton, *J. Am. Chem. Soc.*, **89**, 3158 (1967).
- 19 L. J. Wilson, D. Georges and M. A. Hoselton, *Inorg. Chem.*, **14**, 2969 (1975).
- 20 C. Dabrowiak and D. H. Bush, *Inorg. Chem.*, **14**, 1881 (1975).
- 21 E. Kimura, M. Kodama, R. Machida and K. Ishizu, *Inorg. Chem.*, **21**, 595 (1982).
- 22 J. A. Bauman and T. J. Meyer, *Inorg. Chem.*, **19**, 345 (1980).
- 23 T. R. Weaver, T. J. Meyer, S. Adeyemi, G. M. Brown, R. P. Eckberg, E. C. Johnson, R. W. Murray and D. Untereker, *J. Am. Chem. Soc.*, **97**, 3039 (1975).
- 24 R. R. Gagnè, C. L. Spiro, T. J. Smith, C. A. Hamann, W. R. Thies and A. K. Shiemke, *J. Am. Chem. Soc.*, **103**, 4073 (1981).
- 25 W. M. Coleman, R. K. Boggess, J. W. Hughes and L. I. Taylor, *Inorg. Chem.*, **20**, 700 (1981).
- 26 C. K. Jorgensen, 'Oxidation Numbers and Oxidation States', Springer, New York, 1969.
- 27 L. E. Orgel, *J. Chem. Phys.*, **23**, 1919 (1955).
- 28 J. S. Griffith, *J. Inorg. Nucl. Chem.*, **2** (1) 228 (1956).